

Heavy-to-light meson form factors at large recoil

RICHARD J. HILL

Stanford Linear Accelerator Center, Stanford University

Stanford, CA 94309, U.S.A.

rjh@slac.stanford.edu

Abstract

Heavy-to-light meson form factors at large recoil can be described using the same techniques as for hard exclusive processes involving only light hadrons. Two competing mechanisms appear in the large-recoil regime, describing so-called “soft-overlap” and “hard-scattering” components of the form factors. It is shown how existing experimental data from B and D decays constrain the relative size of these components, and how lattice data can be used to study properties such as the energy scaling laws obeyed by the individual components. Symmetry relations between different form factors (F_+ , F_0 and F_T), and between different heavy initial-state mesons (B and D), are derived in the combined heavy-quark and large-recoil limits, and are shown to generalize corresponding relations valid at small recoil. Form factor parameterizations that are consistent with the large-recoil limit are discussed.

PACS: 12.39.Hg, 12.39.St, 13.20.He, 13.20.Fc

KEYWORDS: Weak decays, B physics, QCD, form factors, symmetry relations

1 Introduction

Form factors for exclusive heavy-to-light meson transitions at large recoil energy, such as $B \rightarrow \pi l \nu$ with $E_\pi \sim m_B/2$, are an important ingredient for measurements of the unitarity triangle, and form the basis for studying more complicated processes such as radiative $B \rightarrow K^* \gamma$ or hadronic $B \rightarrow \pi\pi$ decays. The description of heavy-meson decays into exclusive final states containing energetic light hadrons involves multiple energy scales, and the interplay of perturbative and nonperturbative dynamics. Simplifications arise upon expanding in powers of the heavy-quark mass, m_b , and the light hadron energy, E . The $1/m_b$ expansion, when E is small, is implemented by the heavy-quark effective theory (HQET) [1], while the $1/E$ expansion, when m_b is small, is described by well-known methods for hard-exclusive processes in QCD [2, 3]. The simultaneous expansion for $m_b \sim E \gg \Lambda$, with Λ a typical hadronic scale, requires a merging of these complementary approaches, and results in the soft-collinear effective theory (SCET) [4, 5, 6, 7, 8]. This effective field theory description accomplishes the separation of different energy scales, thus allowing access to the powerful tools of factorization, to relate different processes to universal hadronic quantities, and renormalization, to consistently combine perturbative expansions performed at a high energy scale with the universal nonperturbative quantities evaluated at a low energy scale.

The focus will be on $B \rightarrow P$ transitions, where P is a light (flavor non-singlet) pseudoscalar meson. Matrix elements of the vector and tensor currents are parameterized by the form factors F_+ , F_0 and F_T :

$$\begin{aligned} \langle P(p') | \bar{q} \gamma^\mu b | \bar{B}(p) \rangle &\equiv F_+(q^2) \left(p^\mu + p'^\mu - \frac{m_B^2 - m_P^2}{q^2} q^\mu \right) + F_0(q^2) \frac{m_B^2 - m_P^2}{q^2} q^\mu \\ &\equiv F_+(q^2) (p^\mu + p'^\mu) + F_-(q^2) q^\mu, \\ \langle P(p') | \bar{q} \sigma^{\mu\nu} q_\nu b | \bar{B}(p) \rangle &\equiv \frac{i q^2 F_T(q^2)}{m_B + m_P} \left(p^\mu + p'^\mu - \frac{m_B^2 - m_P^2}{q^2} q^\mu \right), \end{aligned} \quad (1)$$

with $q \equiv p - p'$. The vector form factors F_+ and F_0 are relevant, e.g., in semileptonic $B \rightarrow \pi l \nu$, while the tensor form factor F_T describes, e.g., “penguin” amplitudes in $B \rightarrow K l^+ l^-$. For notational simplicity, results will generally be written for B decays, with the understanding that similar results hold also for D decays with $\bar{B} \leftrightarrow D$ ($b \leftrightarrow c$ at the quark level).

The discussion to follow can be motivated by considering first the case of small recoil, $E \equiv v \cdot p' = m_{Pv} \cdot v' \sim \Lambda$, where the velocities are given by $p^\mu \equiv m_B v^\mu$, $p'^\mu \equiv m_P v'^\mu$. There are two types of form factor relations that arise in the heavy-quark limit [9]. The first type relates different form factors involving the same initial and final states: at leading order in $1/m_b$, the form factors appearing in (1) are related by

$$\frac{F_T(q^2)}{m_B + m_P} = \frac{1}{2m_B} \left[\left(1 + \frac{m_B^2 - m_P^2}{q^2} \right) F_+(q^2) - \frac{m_B^2 - m_P^2}{q^2} F_0(q^2) \right], \quad (2)$$

as follows from (1) upon using $\not{p} b \approx b$. The second type relates form factors involving different initial states, but the same final state (and at the same final-state energy):

$$\frac{F_+^{B \rightarrow P}(E)}{F_+^{D \rightarrow P}(E)} = \sqrt{\frac{m_B}{m_D}}, \quad \frac{F_0^{B \rightarrow P}(E)}{F_0^{D \rightarrow P}(E)} = \sqrt{\frac{m_D}{m_B}}, \quad \frac{m_D + m_P}{m_B + m_P} \frac{F_T^{B \rightarrow P}(E)}{F_T^{D \rightarrow P}(E)} = \sqrt{\frac{m_D}{m_B}}, \quad (3)$$

as follows from again using $\not{v}b \approx b$, and the fact that the left-hand sides in (1) scale as $\sqrt{m_B}$ — the heavy-quark mass is decoupled from the dynamics via a field redefinition, $b(x) = e^{-im_b v \cdot x} h(x) + \dots$, and no other large scales remain.¹ HQET formalizes the $1/m_b$ expansion, making explicit the mass decoupling at leading power and allowing radiative corrections to be systematically incorporated.

Significant modifications should be expected at large recoil for the symmetry relations (2) and scaling laws (3). For instance, the dimensionless parameter $v \cdot v'$ can be as large as $(v \cdot v')_{\max} \approx 6.5$ for semileptonic $D \rightarrow \pi$ transitions, and $(v \cdot v')_{\max} \approx 19$ for $B \rightarrow \pi$. Comparison to a typical dimensionless expansion parameter of HQET, $m_c/\Lambda \sim 3 - 4$ or $m_b/\Lambda \sim 10$, shows that counting $v \cdot v'$ as order unity is likely to lead to a poor expansion, corresponding to neglect of contributions involving the new large scale $\Lambda^2 v \cdot v' \sim E\Lambda$. The regime of applicability for relations such as (2) and (3), and the extent to which significant modifications arise in the kinematic region accessible in B and D decays, was identified as an important question early in the study of heavy-quark hadrons [9, 10], but has so far resisted a quantitative understanding. The present generation of B - and D -decay experiments, as well as lattice gauge-theory simulations, are reaching the level of sensitivity where this question becomes significant (and answerable). The appropriate effective field theory description is now in place to frame this question precisely, and to interpret the relevant data.

There has been considerable attention in the literature directed at the description of heavy-to-light form factors at large recoil. Approaches proceeding in complete analogy with form factors involving only light mesons suffer from the well-known problems associated with endpoint singularities [11, 12]. In [13] it was proposed that the form factors at large recoil should obey symmetry relations appropriate for the transition of a static heavy quark into a light energetic quark, thus avoiding the problem of endpoint singularities by reducing, e.g., all $B \rightarrow \pi$ form factors to a single universal (nonperturbative) function. Symmetry-breaking corrections were investigated in a phenomenological framework in [14], and the effective-theory description of these spectator-interaction effects was initiated in [8]. The form factors have since been studied in more detail using the SCET framework in [15, 16, 17, 18]. This paper shows how these analyses connect to more familiar methods for hard exclusive processes in QCD, derives new symmetry relations at large recoil that generalize (2) and (3), and introduces a convenient parameterization of the form factors for confronting the experimental and lattice data.

The remainder of the paper is organized as follows. In Section 2, the description of form factors in SCET is outlined, and the close connection between the ideas of SCET and the description of hard exclusive processes in QCD is demonstrated. Section 3 presents the resulting symmetry relations that are valid at both small and large recoil. Section 4 introduces a class of parameterizations for the vector $B \rightarrow \pi$ form factors (F_+ and F_0) which accommodate the new terms appearing at large recoil. These new terms require a generalization of parameterizations often used to present experimental and theoretical form-factor results. Section 5 considers the experimental constraints placed on the size of the new terms, and Section 6 compares to recent predictions from lattice QCD and light-cone QCD sum rules. Section 7 provides a concluding discussion.

¹The relativistic normalization of states is used throughout.

2 Form factors in SCET

To make clear the connection with more familiar ideas from the study of hard exclusive processes for light hadrons, it is useful to first consider the description of light meson form factors in the effective field theory language. In particular, the matrix elements of the vector current defining the elastic pion form factor,

$$\langle \pi(p') | \bar{\psi} \gamma^\mu \psi | \pi(p) \rangle \equiv (p^\mu + p'^\mu) F_\pi(q^2), \quad (4)$$

and the $\rho - \pi$ transition form factor,

$$\langle \pi(p') | \bar{\psi} \gamma^\mu \psi | \rho(p, \eta) \rangle \equiv 2i \epsilon^{\mu\nu\rho\sigma} \eta_\nu p_\rho p'_\sigma \frac{F_{\rho\pi}(q^2)}{m_\rho + m_\pi}, \quad (5)$$

capture all of the essential ingredients required to describe large-recoil $B - \pi$ form factors.

The first task is to decompose $\bar{\psi} \gamma^\mu \psi$ into the most general effective-theory operator. Factorization and symmetry properties for the decay amplitude can then be examined at the operator level. In preparation for the discussion of heavy-to-light form factors, the analysis is done in the rest frame of the initial-state meson. To obtain an explicit scale separation, the momentum modes of the quark and gluon fields $\psi(x)$ and $A_\mu(x)$ are grouped into different momentum regions. A separate effective-theory field is assigned to each such region, and the interaction Lagrangian between these effective-theory “particles” is expanded order by order in $1/E$ [4, 5, 6, 7, 8, 19]. The field decomposition is described in terms of light-cone reference vectors n and \bar{n} , satisfying $n^2 = \bar{n}^2 = 0$ and $n \cdot \bar{n} = 2$; e.g, the default choice is $n^\mu = (1, 0, 0, 1)$ and $\bar{n}^\mu = (1, 0, 0, -1)$ for an energetic hadron moving in the z -direction. A general momentum can then be expressed as

$$p^\mu = n \cdot p \frac{\bar{n}^\mu}{2} + \bar{n} \cdot p \frac{n^\mu}{2} + p_\perp^\mu, \quad (6)$$

or more compactly, $p = (n \cdot p, \bar{n} \cdot p, p_\perp)$. The necessary field content of the effective theory involves the soft region, with momentum components of order $p_s \sim E(\lambda, \lambda, \lambda)$; the collinear region, with $p_c \sim E(\lambda^2, 1, \lambda)$; and the soft-collinear region, with $p_{sc} \sim E(\lambda^2, \lambda, \lambda^{3/2})$.² Here $\lambda = \Lambda/E \ll 1$ is a dimensionless expansion parameter. Fields $\mathcal{X}_c, \mathcal{A}_c$ are introduced for collinear particles, and $\mathcal{Q}_s, \mathcal{A}_s$ for soft particles.³ The soft-collinear region, represented by q_{sc} and A_{sc} , describes endpoint configurations of the soft initial-state meson, and collinear final-state meson, where the $n \cdot p$ and $\bar{n} \cdot p$ components of momentum become atypically small [19]. Sensitivity to this region signals a breakdown of factorization, since soft-collinear “messenger” particles may be exchanged between the soft and collinear sectors. Soft-collinear contributions are not perturbatively calculable, so that demonstrating their absence or cancellation to all orders in perturbation theory is a necessary ingredient in establishing factorization for

²An equivalent “moving SCET” description is obtained from the Lorentz boost $n \cdot p \rightarrow \lambda^{-1/2} n \cdot p$, $\bar{n} \cdot p \rightarrow \lambda^{1/2} \bar{n} \cdot p$, under which soft, collinear and soft-collinear become \bar{n} -collinear, $p_{\bar{c}} \sim E'(1, \lambda'^2, \lambda')$; n -collinear, $p_c \sim E'(\lambda'^2, 1, \lambda')$; and ultrasoft, $p_{us} \sim E'(\lambda'^2, \lambda'^2, \lambda'^2)$, respectively [19]. Here $\lambda' = \lambda^{1/2}$ and $E' \sim \sqrt{E\Lambda}$ are the expansion parameter and energy in the boosted frame.

³These fields reduce to the ordinary collinear and soft degrees of freedom (ξ_c, A_c) and (q_s, A_s) in light-cone gauge $\bar{n} \cdot A_c = 0$ and $n \cdot A_s = 0$, but in general contain additional gauge strings to make the operators invariant under soft and collinear gauge transformations.

	d	$[\lambda]$		d	$[\lambda]$
$\frac{1}{\bar{n}\cdot\partial_c}\bar{\mathcal{X}}_c\frac{\not{n}}{2}\Gamma'\mathcal{X}_c$	2	2	$g_{\perp}^{\mu\nu}, \epsilon_{\perp}^{\mu\nu}$	0	0
$\frac{1}{n\cdot\partial_s}\bar{\mathcal{Q}}_s\frac{\not{n}}{2}\Gamma'\mathcal{Q}_s$	2	2	$\partial_{c\perp}^{\mu}, \mathcal{A}_{c\perp}^{\mu}, \partial_{s\perp}^{\mu}, \mathcal{A}_{s\perp}^{\mu}$	1	1
$\bar{\mathcal{Q}}_s\Gamma''\mathcal{Q}_s$	3	3	$n\cdot\partial_s\bar{n}\cdot\partial_s, n\cdot\partial_s\bar{n}\cdot\mathcal{A}_s$	2	2
$n\cdot\partial_s\bar{\mathcal{Q}}_s\frac{\not{n}}{2}\Gamma'\mathcal{Q}_s$	4	4	$\bar{n}\cdot\partial_c n\cdot\partial_c, \bar{n}\cdot\partial_c n\cdot\mathcal{A}_c$	2	2
			$\frac{1}{\bar{n}\cdot\partial_c n\cdot\partial_s}$	-2	-1

Table 1: Boost-invariant building blocks for SCET_{II} operators, with their dimension d and order $[\lambda]$ in the power expansion. Soft derivatives ∂_s can act on any soft field in the operator, collinear derivatives ∂_c on any collinear field. Here $\Gamma' \in \{1, \gamma_5, \gamma_{\perp}^{\mu}\}$, $\Gamma'' \in \Gamma' \cup \{\not{n}, \not{s}, \gamma_{\perp}^{\mu}\gamma_5, \gamma_{\perp}^{\mu}\gamma_{\perp}^{\nu} - \gamma_{\perp}^{\nu}\gamma_{\perp}^{\mu}\}$, $g_{\perp}^{\mu\nu} = g^{\mu\nu} - \frac{1}{2}(\bar{n}^{\mu}n^{\nu} + n^{\mu}\bar{n}^{\nu})$ and $\epsilon_{\perp}^{\mu\nu} = \frac{1}{2}\epsilon^{\mu\nu\alpha\beta}\bar{n}_{\alpha}n_{\beta}$.

a particular process [20, 17, 21]. This cancellation occurs for F_{π} in (4), but not for $F_{\rho\pi}$ in (5). Similarly, the $B \rightarrow \pi$ form factors at large recoil contain both a factorizable and a nonfactorizable piece.

At leading order in $1/Q^2$, where $Q^2 = -q^2 \approx n \cdot p \bar{n} \cdot p' \sim \Lambda E$, the pion form factor (4) is given by

$$F_{\pi} = \frac{1}{Q^2} \langle \pi(p') | [-i\bar{n} \cdot \partial \bar{\psi} \not{n} \psi] | \pi(p) \rangle = \frac{1}{Q^2} \langle \pi(p') | [in \cdot \partial \bar{\psi} \not{n} \psi] | \pi(p) \rangle. \quad (7)$$

In either case, the operator to be represented, $[-i\bar{n} \cdot \partial \bar{\psi} \not{n} \psi]$ or $[in \cdot \partial \bar{\psi} \not{n} \psi]$, has dimension four. The effective-theory representation can be obtained using Table 1 of [21], reproduced here as Table 1.⁴ This table summarizes the building blocks which comprise the general effective-theory operators, including their mass dimension d and power-counting $[\lambda]$. We first consider contributions to the matrix element in (7) from “typical” momentum configurations of the initial-state soft pion, and final-state collinear pion, i.e., configurations in which none of the partons are in atypical endpoint momentum regions. The effective-theory operators must then have the minimal valence field content $\bar{\mathcal{X}}_c(\dots)\mathcal{X}_c\bar{\mathcal{Q}}_s(\dots)\mathcal{Q}_s$, in order to mediate the transition of the soft pion into the energetic collinear pion. Using the table for $d = 4$, the lowest order in power counting at which this field content can be realized is $[\lambda] = 4$. From (7) it follows immediately that

$$F_{\pi} \sim \frac{1}{Q^2}. \quad (8)$$

It can be shown using similar power-counting arguments [21] that the infrared soft-collinear momentum regions are absent at leading power from the matrix elements (7), and that the resulting expression takes a factorized form, in terms of a convergent convolution integral over meson light-cone distribution amplitudes (LCDAs) and a perturbatively calculable hard-scattering kernel.

⁴For a related approach, see [16].

The $\rho - \pi$ form factor (5) is given by

$$\frac{F_{\rho\pi}}{m_\rho + m_\pi} = \frac{1}{Q^2} (-i) \epsilon_{\perp}^{\mu\nu} \eta_\mu^* \langle \pi(p') | [\bar{\psi} \gamma_{\perp\nu} \psi] | \rho(p, \eta) \rangle, \quad (9)$$

with $\epsilon_{\perp}^{\mu\nu}$ as in Table 1. The operator $[\bar{\psi} \gamma_{\perp\nu} \psi]$ has dimension three, and from Table 1, the leading effective-theory operators with $d = 3$ containing the minimal valence field content $\bar{\mathcal{X}}_c(\dots) \mathcal{X}_c \bar{\mathcal{Q}}_s(\dots) \mathcal{Q}_s$ have $[\lambda] = 4$. From (9), it follows immediately that

$$\frac{F_{\rho\pi}}{m_\pi + m_\rho} \sim \frac{1}{Q^4}. \quad (10)$$

The operators in this case involve at least one occurrence of the inverse derivative $(\bar{n} \cdot \partial_{cn} \cdot \partial_s)^{-1}$, as well as transverse derivatives, extra gluon fields, or the occurrence of operators such as $\bar{\mathcal{Q}}_s \Gamma'' \mathcal{Q}_s$ corresponding to subleading-twist wavefunctions of the initial-state meson. Using similar power-counting arguments [21], infrared momentum regions can be shown to contribute at leading power, spoiling factorization between the soft and collinear sectors.

The mode structure and power counting of SCET, as summarized by the building blocks in Table 1, thus naturally reproduce the dimensional/helicity counting rules for hard exclusive processes involving light mesons [2], e.g. (8) and (10). The effective theory also allows all-orders statements concerning factorization to be made; in particular, the well-known factorizable form of F_π at leading order in $1/Q^2$ follows from the uniqueness of the operator with $d = [\lambda] = 4$, together with simple field redefinitions that demonstrate the cancellation of contributions from infrared momentum regions in the matrix element of this operator. The same arguments demonstrate that $F_{\rho\pi}$ is sensitive to infrared momentum regions at leading power, giving rise to the well-known endpoint singularities that appear in this case [22].

The extension to large-recoil heavy-to-light form factors involves one step in addition to the above analysis. Here the heavy-quark mass m_b introduces an additional hard scale into the problem, so that mapping onto the low-energy theory in this case involves first integrating out “hard” scales of order $\mu^2 \sim m_b^2$. The resulting description is then independent of the heavy-quark mass, and the analysis proceeds in direct analogy with the above case, involving only light hadrons, to integrate out the remaining “hard-collinear” scale of order $\mu^2 \sim E\Lambda \sim m_b\Lambda$. The only difference is the novel (HQET) description of the soft heavy quark, obtained by replacing the soft Lagrangian by the HQET Lagrangian, and the soft light-quark field \mathcal{Q}_s by the soft heavy-quark field \mathcal{H}_s . It should be emphasized that this additional step of integrating out the heavy quark can be treated perturbatively, and that the remaining low-energy theory consists of precisely the same momentum modes as for light-meson systems.

The first step of integrating out hard (but not hard-collinear) scales is accomplished by matching QCD onto an intermediate effective theory, denoted SCET_I. This intermediate theory describes hard-collinear and soft fields, with momentum $p_{hc} \sim E(\lambda, 1, \lambda^{1/2})$ and $p_s \sim E(\lambda, \lambda, \lambda)$, respectively. Each SCET_I operator has a well-defined mass dimension, and the matching onto the final effective theory, denoted SCET_{II}, is accomplished by using Table 1 and the same dimensional arguments as above. In particular, for the representation of QCD current operators [23, 18],

$$\bar{q}\Gamma b \rightarrow C_i^A(E, m_b) J_i^A + \frac{1}{2E} \int_0^1 du C_j^B(E, m_b, u) J_j^B(u) + \dots, \quad (11)$$

where the SCET_I operators of dimension three and four have the form

$$J_i^A = \bar{\mathcal{X}}_{hc}(0)\Gamma_i^A h(0),$$

$$J_j^B(u) = \bar{n} \cdot P \int \frac{ds}{2\pi} e^{-ius\bar{n}\cdot P} \bar{\mathcal{X}}_{hc}(s\bar{n}) \mathcal{A}_{hc\perp\mu}(0) \Gamma_j^{B\mu} h(0). \quad (12)$$

Here \mathcal{X}_{hc} and \mathcal{A}_{hc} are hard-collinear quark and gluon fields and h is the heavy-quark field. The reference vectors n and \bar{n} are chosen such that $v_\perp = 0$. At leading power the energy is given by $2E = n \cdot v\bar{n} \cdot P$, where $\bar{n} \cdot P$ is the total large-component of collinear momentum. The quantities u and $(1-u)$ in (12) represent the momentum fractions carried by the quark and gluon fields, respectively. Using Table 1 to match onto operators with minimal field content $\bar{\mathcal{X}}_c(\dots)\mathcal{X}_c\bar{\mathcal{Q}}_s(\dots)\mathcal{H}_s$ shows that large-recoil heavy-to-light meson form factors have two components — one A -type, nonfactorizable, contribution as in the $\rho - \pi$ form factor, and another B -type, factorizable, contribution as in the pion form factor. The complete result at leading power in $1/m_b$ is expressed as [14, 15, 16, 17, 18]

$$F_i^{B \rightarrow M}(E) = \sqrt{m_B} \left[C_{F_i}^A(E, m_b, \mu) \hat{\zeta}_M(E, \mu) \right. \\ \left. + \frac{1}{2E} \int_0^\infty \frac{d\omega}{\omega} \frac{F(\mu)}{4} \phi_+(\omega, \mu) \int_0^1 du f_M(\mu) \phi_M(u, \mu) \int_0^1 du' \mathcal{J}_\Gamma(u, u', \ln \frac{2E\omega}{\mu^2}, \mu) C_{F_i}^B(E, m_b, u', \mu) \right], \quad (13)$$

where M represents the light pseudoscalar (P) or vector (V) final state meson. Since the A -type contribution is nonfactorizable, the SCET_I matrix element is simply defined by⁵

$$\langle M(p) | \bar{\mathcal{X}}_{hc} \Gamma h | B(v) \rangle = -2E \sqrt{m_B} \hat{\zeta}_M(E, \mu) \text{tr} [\bar{\mathcal{M}}_M(n) \Gamma \mathcal{M}(v)], \quad (14)$$

where $\mathcal{M}(v)$ and $\mathcal{M}_M(n)$ are spinor wave-functions appropriate to the heavy-quark and large-energy limits [21]. The light-cone distribution amplitudes for the heavy and light mesons are defined by

$$\langle 0 | \bar{\mathcal{Q}}_s(tn) \frac{\not{n}}{2} \Gamma \mathcal{H}_s(0) | B(v) \rangle = \frac{iF(\mu)}{2} \sqrt{m_B} \text{tr} \left[\frac{\not{n}}{2} \Gamma \mathcal{M}(v) \right] \int_0^\infty d\omega e^{-i\omega tn \cdot v} \phi_+(\omega, \mu),$$

$$\langle M(p) | \bar{\mathcal{X}}_c(s\bar{n}) \Gamma \frac{\not{\bar{n}}}{2} \mathcal{X}_c(0) | 0 \rangle = \frac{if_M(\mu)}{4} \bar{n} \cdot p \text{tr} \left[\bar{\mathcal{M}}_M(n) \Gamma \right] \int_0^1 du e^{ius\bar{n}\cdot p} \phi_M(u, \mu), \quad (15)$$

with associated decay constants $F(\mu)$ and $f_M(\mu)$. Functions C^A and C^B are matching coefficients for the first matching step (QCD onto SCET_I). The “jet function” \mathcal{J}_Γ is the universal matching coefficient for the factorizable B -type contribution in the second matching step (SCET_I onto SCET_{II}), with $\mathcal{J}_\Gamma = \mathcal{J}_\parallel$ for decays to pseudoscalar or longitudinally-polarized vector mesons, and $\mathcal{J}_\Gamma = \mathcal{J}_\perp$ for decays to transversely-polarized vector mesons [18].

The dependence on energy, heavy-quark mass and renormalization scale has been made explicit for the various quantities in (13). In particular, the heavy-quark mass dependence

⁵ $\hat{\zeta}_M$ in (13) and ζ_M in [18] are related by $\zeta_M = \sqrt{m_B} \hat{\zeta}_M$.

enters the large-recoil heavy-to-light form factors only via two sources: the overall factor $\sqrt{m_B}$, simply a result of the relativistic normalization convention for the B -meson state; and the *perturbatively calculable* coefficients C^A and C^B . The energy dependence is also perturbatively calculable for the B -type contribution. Taking $C^B = -1$, and the tree-level jet function,

$$\mathcal{J}_{\parallel}(u, u')_{\text{tree}} = \mathcal{J}_{\perp}(u, u')_{\text{tree}} = -\frac{4\pi C_F \alpha_s}{N} \frac{1}{2E(1-u)} \delta(u - u'), \quad (16)$$

the quantities⁶

$$\hat{H}_M(E, \mu) \equiv \frac{-1}{2E} \int_0^\infty \frac{d\omega}{\omega} \frac{F(\mu)}{4} \phi_+(\omega, \mu) \int_0^1 du f_M(\mu) \phi_M(u, \mu) \int_0^1 du' \mathcal{J}_{\Gamma}(u, u', \ln \frac{2E\omega}{\mu^2}, \mu), \quad (17)$$

to be considered in detail in the following section, are seen to scale exactly as $1/E^2$. Radiative corrections to the jet functions \mathcal{J}_{Γ} , and to the hard matching coefficients C^B , lead to perturbatively calculable violations of this tree-level scaling law. The $1/E^2$ law also follows from the heavy-quark mass dependence in (13), combined with the SCET power counting, $F_i \sim \lambda^{3/2}$, and applies to both the A -type and B -type contributions. However, since the nonperturbative function $\hat{\zeta}_M$ depends on energy, scaling violations for the A -type contributions are not perturbatively calculable.

Both the A -type and B -type components of the form factors in (13) appear at leading power in $1/m_b \sim 1/E$. The two components do not mix under renormalization [18], and it is then a physically meaningful, and phenomenologically important, question which, if either, component is dominant.

3 Symmetry relations in the large-recoil limit

Given the present uncertainty in the hadronic input parameters appearing in (13), it is useful to consider consequences of this description that are independent of these inputs. In the following discussion, coefficients $C_{F_i}^A$ and $C_{F_i}^B$ in (13) will be taken at tree-level. Higher-order radiative corrections are small, and their effects are discussed in Section 7. Because C^B is independent of momentum fraction at tree level, this coefficient can be taken outside of the convolution integral over u' in (13), and the B -type contribution is then described by the universal function, \hat{H}_M , introduced in (17).

The remainder of the paper focuses on the case $M = P$, i.e., decays into pseudoscalar final states. Choosing the normalization of the $B \rightarrow P$ form factors as F_+ , $(m_B/2E)F_0$ and $[m_B/(m_B+m_P)]F_T$, the A -type coefficients are equal to unity at tree level: $C_{F_+}^{A(\text{tree})} = C_{F_0}^{A(\text{tree})} = C_{F_T}^{A(\text{tree})} = 1$. Also with this normalization, the B -type coefficients are $C_{F_+}^{B(\text{tree})} = 1 - 4E/m_B$, $C_{F_0}^{B(\text{tree})} = -1$, and $C_{F_T}^{B(\text{tree})} = 1$. From (13) and (17),

$$F_+(E) = \sqrt{m_B} \left[\hat{\zeta}_P(E) + \left(\frac{4E}{m_B} - 1 \right) \hat{H}_P(E) \right],$$

⁶ \hat{H}_M in (17) and H_M in [18] are related by $H_M = \sqrt{m_B}(m_B/2E)^2 \hat{H}_M$.

$$\begin{aligned}\frac{m_B}{2E}F_0(E) &= \sqrt{m_B} \left[\hat{\zeta}_P(E) + \hat{H}_P(E) \right], \\ \frac{m_B}{m_B + m_P}F_T(E) &= \sqrt{m_B} \left[\hat{\zeta}_P(E) - \hat{H}_P(E) \right].\end{aligned}\tag{18}$$

A residual scale dependence is present in the quantities $\hat{\zeta}_P$ and \hat{H}_P , being cancelled by radiative corrections which have been neglected in the hard-scale coefficients C^A and C^B . For definiteness, $\hat{\zeta}_P(E) \equiv \hat{\zeta}_P(E, \mu = 2E)$ and $\hat{H}_P(E) \equiv \hat{H}_P(E, \mu = 2E)$ in (18). Since the three form factors in (18) are described by only two functions, there is one nontrivial relation between them [18, 24]:⁷

$$\frac{m_B}{m_B + m_P} \frac{q^2}{m_B^2} F_T(E) = F_+(E) - F_0(E).\tag{19}$$

For comparison, we may rewrite (2), dropping kinematic factors quadratic in the light-meson mass, as

$$\frac{m_B}{m_B + m_P} \frac{q^2}{m_B^2} F_T(E) = F_+(E) - F_0(E) - \frac{1}{2} \left[\frac{2E}{m_B} F_+(E) - F_0(E) \right].\tag{20}$$

Since the extra terms in (20) involve factors, E/m_B or F_0/F_+ , that are suppressed at small recoil, both (19) and (20) are valid relations at leading power in this regime. However, at large recoil the extra terms involving \hat{H}_P are not suppressed, and here (19) is the correct relation. It is interesting to note that if the terms involving \hat{H}_P are neglected, then the relation (2) (or (20)) derived at small recoil is seen to hold in the full kinematic range. Form factors describing B decays to vector final states exhibit the same behavior: the relations derived at small-recoil are equivalent to relations valid at large recoil, plus hard-scattering corrections. In the regime $E \sim m_b \gg \Lambda$, both $\hat{\zeta}_P$ and \hat{H}_P are of the same order in power counting, and only a numerical, but not parametric, suppression could justify neglecting one or the other term. In fact, when $E \gg m_b \gg \Lambda$ (an energy regime beyond that accessible in B decays), the hard-scattering terms dominate, as seen from the fact that the B - π form factor must be described at leading order in $1/E$ in the same way as the π - π form factor (cf. (7) and (8) above), but with an asymmetric B -meson wavefunction replacing the initial-state pion wavefunction. It is precisely the cross-over regime $E \sim m_b$, where both components are of the same order, that is most relevant to experimental studies in B -decays.

As in the case of small recoil, heavy-quark symmetry may be used to relate form factors at large recoil for different heavy mesons. From (18),

$$\frac{F_-^{B \rightarrow P}(E)}{F_-^{D \rightarrow P}(E)} = \sqrt{\frac{m_B}{m_D}}, \quad \frac{F_0^{B \rightarrow P}(E)}{F_0^{D \rightarrow P}(E)} = \sqrt{\frac{m_D}{m_B}}, \quad \frac{m_D + m_P}{m_B + m_P} \frac{F_T^{B \rightarrow P}(E)}{F_T^{D \rightarrow P}(E)} = \sqrt{\frac{m_D}{m_B}},\tag{21}$$

⁷In [7] it was shown that with tree-level matching there are no contributions from $\mathcal{O}(\lambda^{1/2})$ SCET_I operators that violate the relation (19). Since dimensional analysis and power-counting [16, 21] shows that no $\mathcal{O}(\lambda)$ SCET_I operators can match onto SCET_{II} operators giving leading-order form-factor contributions, the result (19) then follows. Note however that the converse is not true - although the symmetry relations for vector final states, between form factors V and A_1 , and between T_1 and T_2 , receive contributions from $\mathcal{O}(\lambda^{1/2})$ SCET_I operators [7], these corrections are of higher order in the final SCET_{II} power counting, leaving exact relations at leading power [18].

with F_- defined in (1). Both (3) and (21) are valid relations at small recoil, where $(F_- + F_+)/F_+ \sim 1/m_b$. However, at large recoil the terms involving \hat{H}_P enter at leading power, and here (21) gives the correct relations.

4 Form factor parameterizations and the large-recoil limit

The form factor of primary phenomenological interest for $B \rightarrow \pi$ decays is F_+ , since (for massless leptons), it is the only form factor required to extract $|V_{ub}|$ from the experimental $B \rightarrow \pi l \nu$ rate. Due to the kinematic constraint $F_+ = F_0$ at $q^2 = 0$, it is useful to consider also F_0 , in order to help constrain extrapolations of form factor determinations at small recoil into the large recoil regime. It will be convenient to introduce the following normalization and shape parameters describing these two form factors at large recoil:

$$f(0) \equiv F_+(0), \quad \delta \equiv 1 + \frac{F_-(0)}{F_+(0)}, \quad \frac{1}{\beta} \equiv \frac{m_B^2 - m_\pi^2}{F_+(0)} \frac{dF_0}{dq^2} \Big|_{q^2=0}. \quad (22)$$

From the definition of F_- , it follows immediately from (22) that

$$\frac{m_B^2 - m_\pi^2}{F_+(0)} \left(\frac{dF_+}{dq^2} \Big|_{q^2=0} - \frac{dF_0}{dq^2} \Big|_{q^2=0} \right) = 1 - \delta. \quad (23)$$

Thus the relative *normalization* of F_+ and F_0 is fixed at maximum recoil by the kinematic constraint

$$F_+(q^2 = 0) = F_0(q^2 = 0), \quad (24)$$

while the relative *slope* of F_+ and F_0 is determined by the quantity δ . In addition to the quantities (22) referring to the large-recoil behavior of the form factors, it is convenient to introduce the following parameters describing the form factors at small recoil:

$$\frac{1}{1 - \alpha} \equiv \frac{1}{m_{B^*}^2} \text{Res}_{q^2=m_{B^*}^2} \frac{F_+(q^2)}{F_+(0)}, \quad f(m_B^2) \equiv F_0(m_B^2). \quad (25)$$

Note that although the notation anticipates the parameterizations to be discussed below, the quantities α , β , δ , $f(0)$ and $f(m_B^2)$ have been introduced simply as convenient definitions for the exact physical quantities appearing on the right-hand sides in (22) and (25).

The parameters $(f(0), \alpha, \beta, \delta)$ are sufficient to describe the present generation of experimental and lattice form factor data. Additional shape parameters can be introduced to obtain a systematically improved form factor parameterization. A straightforward approach starts from the dispersive representation,

$$F_+(q^2) = \frac{F_+(0)/(1 - \alpha)}{1 - q^2/m_{B^*}^2} + \frac{1}{\pi} \int_{(m_B+m_\pi)^2}^{\infty} dt \frac{\text{Im}F_+(t)}{t - q^2},$$

$$F_0(q^2) = \frac{1}{\pi} \int_{(m_B+m_\pi)^2}^{\infty} dt \frac{\text{Im}F_0(t)}{t - q^2}, \quad (26)$$

where the B^* pole appears in F_+ as a distinct contribution below the $B\pi$ threshold. A series of increasingly precise approximations to the form factors in the semileptonic region, $0 < q^2 < (m_B - m_\pi)^2$, is obtained by breaking up the integrals in (26), and is given for increasing N by

$$\begin{aligned} F_+ &= \frac{f(0)/(1-\alpha)}{1 - \frac{q^2}{m_{B^*}^2}} + \frac{\rho_1}{1 - \frac{1}{\gamma_1} \frac{q^2}{m_{B^*}^2}} + \dots + \frac{\rho_N}{1 - \frac{1}{\gamma_N} \frac{q^2}{m_{B^*}^2}}, \\ F_0 &= \frac{\kappa_1}{1 - \frac{1}{\beta_1} \frac{q^2}{m_{B^*}^2}} + \dots + \frac{\kappa_N}{1 - \frac{1}{\beta_N} \frac{q^2}{m_{B^*}^2}}, \end{aligned} \quad (27)$$

with parameters constrained by (23) and (24). The main focus will be on the case $N = 1$, which can be written [25]

$$F_+(q^2) = \frac{f(0) \left(1 - \frac{\frac{1}{\gamma} - \alpha}{1 - \alpha} \frac{q^2}{m_{B^*}^2}\right)}{\left(1 - \frac{q^2}{m_{B^*}^2}\right) \left(1 - \frac{1}{\gamma} \frac{q^2}{m_{B^*}^2}\right)}, \quad F_0(q^2) = \frac{f(0)}{1 - \frac{1}{\beta} \frac{q^2}{m_{B^*}^2}}, \quad (28)$$

where the constraints (23) and (24) have been used, and where⁸

$$\frac{1}{\gamma} \equiv 1 - \frac{1 - \alpha}{\alpha} \left(\frac{1}{\beta} - \delta\right). \quad (29)$$

If the experimental or lattice form factor data can be described by (28), then the fit parameters ($f(0), \alpha, \beta, \delta$) yield a determination of the physical quantities describing the form factors — at large recoil on the right-hand sides of (22), and at small recoil on the right-hand sides of (25).

The discussion so far has not required, nor utilized, the large-recoil, heavy-quark expansion of the form factors. From (18), the following relations hold at leading order in $1/m_b$ and $\alpha_s(m_b)$:

$$\begin{aligned} f(0) &= \sqrt{m_B} (\hat{\zeta}_\pi + \hat{H}_\pi) \Big|_{E=m_B/2} + \dots, & \delta &= \frac{2\hat{H}_\pi}{\hat{\zeta}_\pi + \hat{H}_\pi} \Big|_{E=m_B/2} + \dots, \\ \frac{1}{\beta} &= -\frac{d \ln(\hat{\zeta}_\pi + \hat{H}_\pi)}{d \ln E} \Big|_{E=m_B/2} - 1 + \dots \end{aligned} \quad (30)$$

The relations (30), between the physical form factors appearing in (22) and the SCET functions $\hat{\zeta}_\pi$ and \hat{H}_π , are independent of any parameterization. The dependence of the parameters on the heavy-quark mass is determined by the scaling laws $\hat{\zeta}_\pi \sim \hat{H}_\pi \sim 1/E^2$. In particular, $f(0) \sim m_b^{-3/2}$, so that $F_+^{B \rightarrow \pi}(0)/F_+^{D \rightarrow \pi}(0) \approx (m_D/m_B)^{3/2}$. The simple power-counting rules of SCET provide a formal demonstration of this scaling law, which was justified in [25] using more qualitative arguments based on QCD sum rules [26, 13]. Parameter δ is $\mathcal{O}(1)$ in the power

⁸Numerical factors $m_{B^*}^2/m_B^2 - 1$ and m_π^2/m_B^2 are beyond the current level of precision and have been neglected.

counting, and is independent of the heavy-quark mass when scaling violations are neglected. Finally, $\beta - 1 \sim m_b^{-1}$. There are also constraints appearing from the small-recoil regime. Using soft-pion relations, it follows that [27, 28]

$$\frac{f(0)}{1 - \alpha} = \frac{f_{B^*} g_{B^* B \pi}}{2m_{B^*}}, \quad f(m_B^2) = \frac{f_B}{f_\pi}, \quad (31)$$

where f_π , f_B and f_{B^*} are decay constants, and $g_{B^* B \pi}$ is the coupling of the B and B^* mesons to the pion. If this coupling, and/or the decay constants for the B and B^* mesons were determined precisely, they could be used to place further constraints on the parameters appearing in (28), or the more general parameterization (27). Conversely, to the extent that the data is described by (28), the resulting fit parameters provide a determination of $f_{B^*} g_{B^* B \pi}$ and f_B . The analysis in Sections 5 and 6 concentrates on the region $\alpha < 1$, as required for $f(0) > 0$, $g_{B^* B \pi} > 0$. Power counting in (31) at small recoil, together with the scaling law $f(0) \sim m_b^{-3/2}$, implies that $\alpha - 1 \sim m_b^{-1}$ and $f(m_B^2) \sim m_b^{-1/2}$. The quantity γ in (29) is then given up to corrections of order $1/m_b^2$ by

$$\frac{1}{\gamma} = \alpha + \delta(1 - \alpha), \quad (32)$$

yielding the parameterization:

$$F_+(q^2) = \frac{f(0) \left(1 - \delta \frac{q^2}{m_{B^*}^2}\right)}{\left(1 - \frac{q^2}{m_{B^*}^2}\right) \left(1 - [\alpha + \delta(1 - \alpha)] \frac{q^2}{m_{B^*}^2}\right)}, \quad F_0(q^2) = \frac{f(0)}{1 - \frac{1}{\beta} \frac{q^2}{m_{B^*}^2}}. \quad (33)$$

Due to the different energy dependence of the coefficients multiplying $\hat{\zeta}_P$ and \hat{H}_P in (18), information on the parameter δ describing the relative size of $\hat{\zeta}_P$ and \hat{H}_P can be extracted from the single form factor, F_+ , that is most readily accessible experimentally.⁹ Several special limits of F_+ in (33) may be noted. Firstly, points on the line $\delta = 1$ or on the line $\alpha = 0$ are equivalent and correspond to the simple pole model, with a single pole at $q^2 = m_{B^*}^2$. Secondly, the ‘‘point-at-infinity’’, given by $\alpha \rightarrow \infty$, $\delta \rightarrow 1$ with $\alpha(1 - \delta)$ fixed, corresponds to a single pole model, with pole at $q^2 = m_{B^*}^2/[1 + \alpha(1 - \delta)]$. If the physical values of the shape parameters were to lie close to one of these special points, then the parameter choice (γ, δ) , with γ from (32), may be more suitable than the choice (α, δ) for performing fits; assuming $\alpha > 0$ and $\delta < 1$, as indicated by the data, this will not be the case. Finally, the axis $\delta = 0$ corresponds to the three-parameter Becirevic-Kaidalov (BK) parameterization [25]. It may also be noted that at small $q^2/m_{B^*}^2$ the shape of F_+ is similar to that of (33) at $\delta = 0$, but with an effective $\alpha_{\text{eff}} = \alpha(1 - \delta)$. Data with sensitivity mostly at small q^2 is therefore not easily distinguished from the three-parameter BK form. In this situation, since $\alpha = 1$ in the heavy-quark limit, a large deviation of α_{eff} from unity could signal a nonzero value of δ . However, with precise enough data, the general form (33) can be distinguished from the $\delta = 0$ case, and the parameter δ measured directly. The analysis in Sections 5 and 6 concentrates on the region $\delta > 0$, corresponding to a positive inverse moment of the B -meson LCDA in (17).

⁹The same could not be done from F_0 , since here both terms behave as E^{-1} at large energy. This fact allows F_0 , but not F_+ , to be modeled by a single pole.

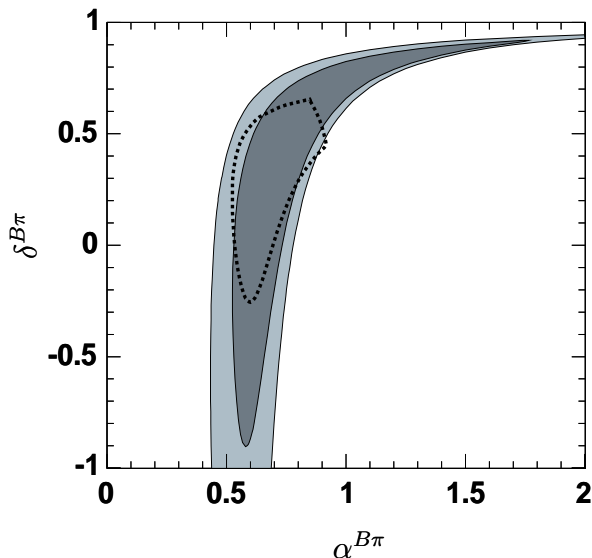


Figure 1: 68% (dark) and 90% (light) confidence regions for parameters α and δ as determined by fitting F_+ in (33) to binned $B \rightarrow \pi l \nu$ branching fraction measurements in [29], [30] and [31]. Also shown is the boundary of the 68% confidence region (dashed line) for the parameterization of F_+ in (28), with $\beta^{B\pi} = 1.2$.

5 Experimental Constraints

Existing experimental data can be used to put significant constraints on the observables defined in (22) and (25). Figure 1 shows the constraints imposed on α and δ by combined CLEO [29] (three q^2 bins), Belle [30] (three q^2 bins) and BaBar [31] (five q^2 bins) $B \rightarrow \pi$ branching fraction measurements. The contours in Figure 1 are obtained from a χ^2 fit of F_+ in (33) to the data, and correspond to 68% ($\Delta\chi^2 = 2.3$) and 90% ($\Delta\chi^2 = 4.6$) confidence-level regions. Systematic errors are added to the statistical errors in quadrature. With the exception of [29], where error correlations between different q^2 bins are available, branching fractions for different bins are assumed uncorrelated, as are the measurements of different experiments. The fit yields $\alpha^{B\pi} = 0.8_{-0.2}^{+0.5}$ and $\delta^{B\pi} = 0.6_{-0.7}^{+0.3}$ as the 68% confidence intervals for the separate parameters. The simple pole model, corresponding to the boundaries of the plot at $\alpha = 0$ and $\delta = 1$, is ruled out decisively by the data (99.99% level). However, the single pole model is not ruled out with high confidence. The contours in Figure 1 thus extend as fine filaments toward the “point-at-infinity” as discussed after (33). If δ is small, power-suppressed terms in α and β may compete with this parameter in (29). For comparison, the 68% confidence-level region obtained from a fit to F_+ in the parameterization (28), before expanding in $\alpha - 1$ and $\beta - 1$, is also shown in Figure 1, using $\beta^{B\pi} = 1.2$ [34, 35] (see Section 6), and imposing the physical constraint $0 < 1/\gamma < m_{B^*}^2/(m_B + m_\pi)^2$ on the position of the effective pole. With

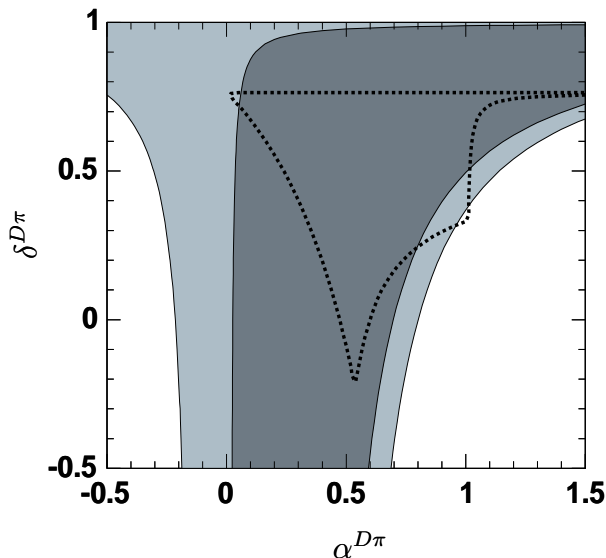


Figure 2: 68% (dark) and 90% (light) confidence regions for parameters α and δ as determined by fitting F_+ in (33) (with $m_{B^*} \rightarrow m_{D^*}$) to $D \rightarrow \pi$ data in [32]. Also shown is the 68% confidence region (dashed line) using the parameterization of F_+ in (28) before expansion, with $\beta^{D\pi} = 1.6$.

the constraint in place, the unexpanded fit yields $1 + 1/\beta^{B\pi} - \delta^{B\pi} = 1.3_{-0.1}^{+0.4}$ ¹⁰.

Treating the charm mass as sufficiently heavy to perform the large-recoil/heavy-quark expansion, the same reasoning as led to (33) yields a similar parameterization for $D \rightarrow \pi$ form factors, with m_{D^*} replacing m_{B^*} . Under the identification (30), and neglecting scaling violations, parameter δ is independent of the heavy-quark mass, and is therefore the same for B and D mesons in the heavy-quark limit. Figure 2 shows constraints imposed by $D \rightarrow \pi l \nu$ data from the CLEO collaboration, which measured relative branching fractions in three q^2 bins [32]. The figure shows 68% and 90% confidence regions for α and δ using the parameterization of F_+ in (33), with $m_{B^*} \rightarrow m_{D^*}$. Also shown is the 68% confidence region for the parameterization of F_+ in (28) before expansion, using $\beta^{D\pi} = 1.6$ [37],¹¹ and imposing the constraint $0 < 1/\gamma < m_{D^*}^2/(m_D + m_\pi)^2$ on the position of the effective pole. With the constraint in place, the unexpanded fit yields $1 + 1/\beta^{D\pi} - \delta^{D\pi} = 1.1_{-0.2}^{+0.6}$.

The same analysis can be performed for $D \rightarrow K$ form factors, with now the D_s^* mass being used in (33). In the limit of exact $SU(3)$ flavor symmetry, parameters α and δ are the same for this case as for $D \rightarrow \pi$ form factors. The CLEO collaboration has measured relative branching fractions for $D \rightarrow K l \nu$ in three q^2 bins [32]. The FOCUS collaboration has extracted the form factor F_+ for $D \rightarrow K \mu \nu$ decays at nine q^2 points [33]. Figure 3 shows a fit of F_+ in (33), with

¹⁰For a more detailed analysis using the general parameterization (27), see [42].

¹¹From the central value for the single-pole fit in [37], $\beta^{D\pi} = [m_{D^*}^2/(m_D^2 - m_\pi^2)] \times 1.41 \approx 1.6$, and $\beta^{DK} = [m_{D_s^*}^2/(m_D^2 - m_K^2)] \times 1.31 \approx 1.8$.

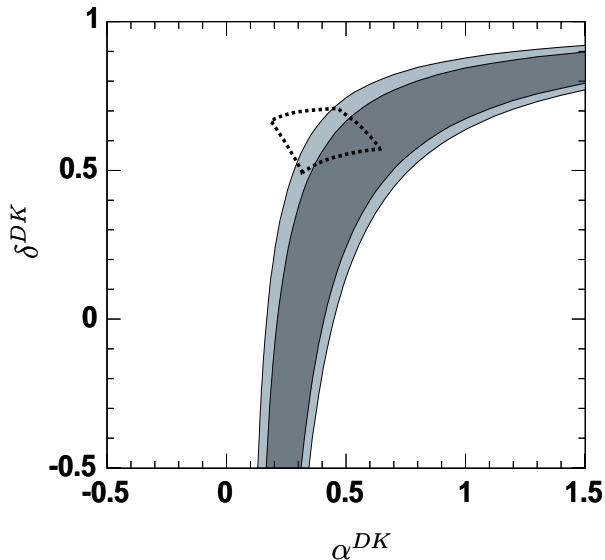


Figure 3: 68% (dark) and 90% (light) confidence regions for parameters α and δ as determined by fitting F_+ in (33) (with $m_{B^*} \rightarrow m_{D_s^*}$) to $D \rightarrow K$ data in [32] and [33]. Also shown is the 68% confidence region (dashed line) using the parameterization of F_+ in (28) before expansion, with $\beta^{DK} = 1.8$.

$m_{B^*} \rightarrow m_{D_s^*}$, to the combined data, again with 68% and 90% confidence regions. The χ^2 fit uses the correlation coefficients from [32] and [33] for the respective data, with the different experiments assumed uncorrelated. The simple pole model ($\alpha = 0$ or $\delta = 1$) is ruled out decisively by the data. The single pole model ($\alpha \rightarrow \infty, \delta \rightarrow 1$ with $\alpha(1 - \delta)$ fixed) is not ruled out with high confidence. Also shown is the 68% confidence region for the parameterization of F_+ in (28) before expansion, using $\beta^{DK} = 1.8$ [37], and imposing the physical constraint $0 < 1/\gamma < m_{D_s^*}^2/(m_D + m_K)^2$ on the position of the effective pole. With the constraint in place, the unexpanded fit yields $1 + 1/\beta^{DK} - \delta^{DK} = 0.91_{-0.05}^{+0.12}$. A direct measurement of the quantity δ (as defined in (22)) in [33] yields $\delta^{DK} = -0.7 \pm 1.5 \pm 0.3$.

6 Comparison to Theoretical Predictions

Explicit theoretical form-factor calculations are important, most notably for supplying the overall normalization necessary to extract weak-interaction parameters ($|V_{ub}|$) from experimental data ($B \rightarrow \pi l \nu$). The form factor shape can be tested independently of this normalization, and also contains important information relating to other processes. Figure 4 shows allowed parameter regions obtained by fitting recent unquenched $B \rightarrow \pi$ lattice data for F_+ and F_0 , from [34] and [35], to (28), imposing the physical constraint $0 < 1/\gamma < m_{B^*}^2/(m_B + m_\pi)^2$ and $0 < 1/\beta < m_{B^*}^2/(m_B + m_\pi)^2$ on the positions of the effective poles. Also shown is the central

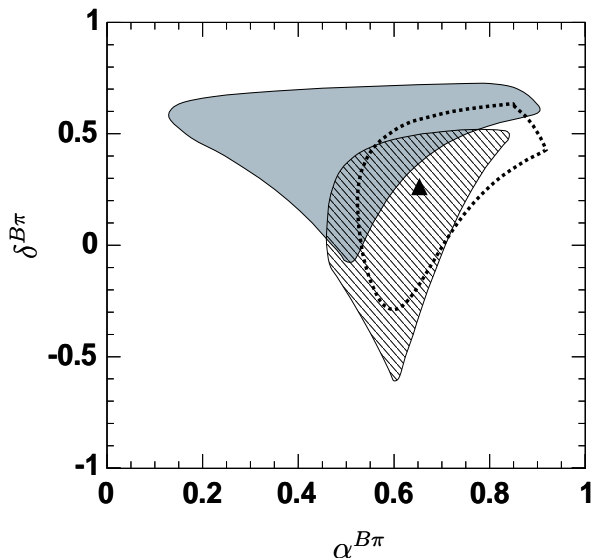


Figure 4: Theoretical constraints on form-factor shape parameters. Shown are 68% confidence regions for parameters α and δ for $B \rightarrow \pi$ as determined by fitting (28) to unquenched lattice QCD in [34] (light solid) and [35] (hatched). The triangle indicates the central value from light-cone sum rules in [36]. Superimposed is the 68% confidence region (dashed line) from experimental data (see Figure 1).

value for the light-cone sum rule determination from [36]. Superimposed is the region preferred by the experimental data, as in Figure 1. It may be noted that the lattice determination of $F_+(q^2)$ in [35] employs the BK parameterization, (33) with $\delta = 0$, to interpolate and extrapolate the data points at varying light-quark mass to fixed energy prior to performing the chiral extrapolation to the physical light-quark mass. Similarly, a single pole model is used in [34] to interpolate to fixed energy before chiral extrapolation. Achieving greater precision warrants further investigation into whether the form assumed for this extrapolation biases the resulting chirally-extrapolated form factors. Also, as a result of fitting to a smooth curve prior to chiral extrapolation, the data points for $F_{+,0}(q^2)$ from [34] and [35] lie on a smooth curve, introducing significant correlations between different q^2 values. The χ^2 fit employed in Figure 4 assumes uncorrelated errors, with statistical and systematic errors added in quadrature.

Under the assumption of the dimensional scaling laws $\hat{\zeta}_\pi \sim 1/E^2$ and $\hat{H}_\pi \sim 1/E^2$, the identification (30) allows the relative size of $\hat{\zeta}_\pi$ and \hat{H}_π to be probed by measuring the single form factor F_+ , using (18). By measuring both F_+ and F_0 , it is possible to isolate the $\hat{\zeta}_\pi$ and \hat{H}_π components directly, and to test this scaling law. With the form factors parameterized according to (28), small deviations of α and β from unity allow for violations of the exact $1/E^2$ scaling that is recovered when $\alpha = \beta = 1$ (for any value of δ). Figure 5 shows the range of slopes for typical parameter values. Parameter β is varied between 1.1 and 1.3; this

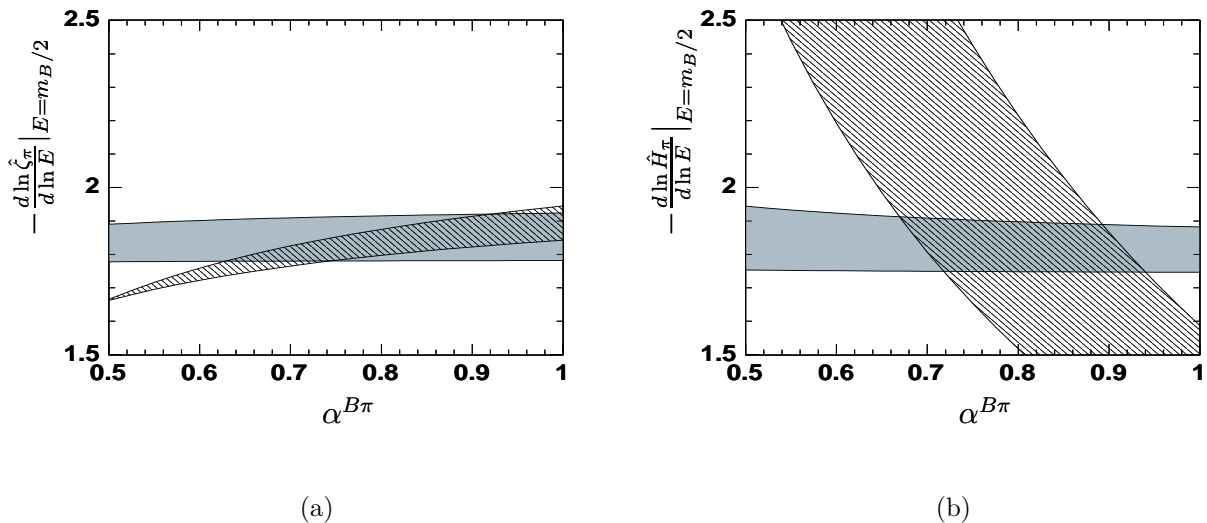


Figure 5: Slope of $\hat{\zeta}_\pi$ (5(a)) and \hat{H}_π (5(b)) at maximum recoil, with F_+ and F_0 given by (28), as a function of α . The hatched region is for $\delta = 0.2$, and the solid region for $\delta = 0.7$. The vertical range within each region corresponds to varying β from $\beta = 1.1$ to $\beta = 1.3$.

is consistent with the lattice values¹² 1.18(5) from [34] and 1.18(5) from [35], and also with the light-cone sum rule result 1.20 from [36]. The magnitude of the slope for ζ_π in Figure 5(a) is slightly below 2 for all parameter values, whereas for \hat{H}_π the result shown in Figure 5(b) depends more sensitively on the value of δ . Small deviations from the $1/E^2$ dimensional scaling law lend confidence to the large-recoil expansion.

7 Discussion

Form factors at large recoil energy are essential to the study of heavy meson decays to exclusive final states. The additional energy scale provided by the heavy quark complicates the description of these processes relative to the case of exclusive processes involving only light hadrons. However, in the minimal effective theory (SCET₁) obtained after integrating out the heavy-quark mass, the description follows that of the light-hadron case, with a novel HQET field replacing one of the light-quark fields. The problem can be made to look more symmetric by boosting to the Breit frame for the light degrees of freedom. In continuum field theory the SCET and “moving SCET” descriptions are of course equivalent; however, in lattice simulations, the maximum light-meson energy in the Breit frame, $E' \sim \sqrt{E\Lambda}$, is much smaller than that in the rest frame of the initial-state heavy meson. The resulting discretization requires far fewer lattice sites to obtain a given accuracy, and can lead to much more efficient simulations. This philosophy lies behind the idea of “moving nonrelativistic QCD” and related

¹²The fits in [34] and [35] assumed $\delta = 0$, but the value of β is not significantly changed by allowing $\delta \neq 0$.

approaches [38], which may allow direct simulations of form factors over most or all of the full kinematic range in $B \rightarrow \pi l \nu$.

Knowledge of the heavy-quark mass dependence of the form factors, and of the relations between different form factors, provides a valuable handle that can be used to test lattice or other theoretical calculations. For example, if F_T were calculated on the lattice, (19) is a model-independent relation that must be satisfied throughout the entire kinematic range. If the hard-scattering contributions are significant, then there is a nontrivial modification at large recoil compared to the corresponding HQET relation (2).

Symmetry relations between form factors for B and D mesons near the kinematic endpoint for D decay can provide a normalization for the B -decay form factors. Relations (21) are valid throughout the entire kinematic range; again, if the hard-scattering contributions are significant, there is a nontrivial modification from the corresponding HQET relations (3). The analysis of B decays to vector final states reveals similar modifications at large recoil to the HQET scaling laws and symmetry relations; a preliminary discussion was given in [24], and a more in-depth analysis is left for future work. Precision measurements would require a detailed study of power corrections, in particular an analysis of the manner in which HQET power corrections [39] merge with the SCET description; this topic is beyond the scope of the present work. However, it should be emphasized that, even at leading order in the heavy-quark expansion, no formal relation exists between form factors $F_+^{B \rightarrow \pi}$ and $F_+^{D \rightarrow \pi}$ near maximum recoil in the $D \rightarrow \pi$ system.

Neglecting scaling violations (and power corrections), the large-recoil scaling laws imply $F_+^{B \rightarrow \pi}(q^2 = 0) = (m_D/m_B)^{3/2} F_+^{D \rightarrow \pi}(q^2 = 0)$. As emphasized in Section 2, the energy dependence of the hard-scattering part of the form factors is calculable; for this part, a full renormalization-group analysis including first-order radiative corrections was performed in [18], using a model B -meson wavefunction. Scaling violations were found to give a small additional suppression for increasing energy relative to the $1/E^2$ tree-level scaling. For the soft-overlap part of the form factors, however, the energy dependence is not perturbatively calculable. Scaling violations for such nonfactorizable quantities provide an interesting window on nonperturbative QCD dynamics. Although for practical purposes, this interesting dynamics can fortunately be avoided through the use of symmetry relations, further direct analysis of $\hat{\zeta}_\pi$ is warranted.

The description in Section 3 used the tree-level approximation for the hard-scale matching coefficients in the effective theory. Like the HQET relations (2) and (3), the SCET form factor relations (19) and (21) receive corrections at $\mathcal{O}(\alpha_s)$, arising as nontrivial matching coefficients of QCD onto the effective theory at the hard matching scale. These radiative corrections have been calculated to first order in α_s , for C^A in [5, 40], and for C^B in [40, 41]. The corrections could be taken into account trivially for the A -type terms; however, since the modifications are $\lesssim 5\%$ for all $B \rightarrow \pi$ form factors [41], they can be safely neglected at the current level of precision. Corrections to C^B are more difficult to quantify, since beyond tree level these coefficients are momentum-fraction dependent, and so knowledge of the shape of the meson wavefunctions becomes necessary. However, these corrections are $\lesssim 20\%$ for all $B \rightarrow \pi$ form factors [41]; if, as the data indicate, the hard-scattering terms (\hat{H}) are significantly smaller than the soft-overlap terms ($\hat{\zeta}$), then the effect on the overall form factors is much smaller. Until evidence of the hard-scattering terms is first seen unambiguously and their properties

can be studied further, this approximation is sufficient.

The parameterization (33) provides a generalization of several forms commonly used in studying form factors for heavy-to-light transitions such as $B \rightarrow \pi$. It is the most general form of F_+ with a pole at $q^2 = m_{B^*}^2$ and one additional effective pole. The simple pole (one pole at $m_{B^*}^2$) and single pole (one pole, not necessarily at $m_{B^*}^2$) models are contained as special cases. Given that the lattice and experimental data cannot yet resolve more than a single effective pole, branching fraction fits and the resulting V_{ub} determinations should be very insensitive to the inclusion of even more terms in (27). In particular, with the asymptotic behavior $F_+(t) \sim 1/t$ at large t , the dispersive integral in (26) is absolutely convergent. This bounds the magnitude of residues ρ_i in (27), and prevents contributions from arbitrarily large t . A more formal study of the convergence properties of the sequence of parameterizations (27) will be taken up elsewhere [42]. Using the identification (30), it follows that specialization to the case $\delta = 0$ in (33), as in [25], corresponds to neglect of the hard-scattering component of the form factor, and is justified only to the extent that this component is shown to be small. Similar parameterizations can be used in $D \rightarrow \pi$, and in $D \rightarrow K$ decays, with the D^* , and D_s^* pole replacing the B^* pole. It would be especially interesting to fix the value of $\delta = 1 + F_-(0)/F_+(0)$ in $D \rightarrow \pi$ decays. From the identifications (30), this quantity is independent of the heavy-quark mass at leading power, and neglecting scaling violations. Since δ is at most a slowly-varying function of the heavy-quark mass, determination of its value for $D \rightarrow \pi$ would give an important indication of its size for $B \rightarrow \pi$.

A related decomposition of the dispersive integral (26) was studied in [43], where a parameterization in terms of explicit resonance and continuum contributions was put forward. The semileptonic data can now be used to test such models — e.g., $B \rightarrow \pi$ (Figure 1) and $D \rightarrow K$ (Figure 3) data definitively resolve contributions other than the B^* and D_s^* pole terms, respectively, and $D \rightarrow \pi$ (Figure 2) data favors contributions in addition to the D^* pole, as indicated by $\alpha > 0$.

A detailed analysis of heavy-to-light form factors provides the basis for more complicated radiative and hadronic B decays. For instance, at leading order in $1/m_b$, $B \rightarrow \pi\pi$ decays can be related via factorization theorems to $B \rightarrow \pi$ form factors, plus hard-scattering corrections [44, 45]. Written in SCET language, the leading-order description is in terms of the same functions $\hat{\zeta}_\pi$ and \hat{H}_π appearing in the form factors [46]. Knowledge of the parameter δ in (18) should help in understanding these more complicated processes, where values ranging from $\delta \sim 0.1 - 0.5$ [47, 48] to $\delta \sim 1.1 - 1.4$ [46, 49] have been taken as phenomenological input or suggested from fits to the $B \rightarrow \pi\pi$ data. The size and nature of power corrections also warrants further investigation [50].

More generally, the value of δ should help in deciding between different schools of thought that have emerged to describe $B \rightarrow \pi$ form factors. The first of these may be conveniently labelled as the “soft-overlap dominance” school, where δ is small, and the hard-scattering terms at large recoil give small corrections to the symmetry relations derived at small recoil; the second, “hard-scattering dominance”, school of thought, where δ is large, assumes that the $B \rightarrow \pi$ transition can be treated in much the same way as for light-meson form factors, where hard-scattering terms are dominant and endpoint contributions are suppressed. Light-cone sum rules generally belong to the first school, where the hard-scattering terms appear as a radiative correction [51, 52, 53]. Some care is required in categorizing various approaches in

the second school, due to different terminologies. In SCET, it is natural to identify the “soft-overlap” contribution with the “nonfactorizable” $\hat{\zeta}$, arising from the “*A*-type” SCET_I current, and satisfying “spin-symmetric” relations (14) appropriate for this leading-order current operator. Similarly, the “hard-scattering” contribution is identified with \hat{H} , and is synonymous with “factorizable”, “*B*-type” and “symmetry-breaking”. Since $\hat{\zeta}$ involves contributions from hard gluon exchange in addition to true soft-overlap contributions from endpoint configurations, dominance of hard-gluon exchange is not necessarily the same as dominance of \hat{H} over $\hat{\zeta}$. The numerical value of δ provides a useful and unambiguous means of comparing the implications of different approaches.

The heavy-quark expansion for exclusive heavy-meson decay amplitudes yields results such as the well-known symmetry relations between different form factors, and between different heavy mesons, which are strictly valid when no other large energy scales are relevant. For decays into energetic hadrons, hard-scattering contributions involving the spectator degrees of freedom in the heavy meson involve such a new large scale, whose effects may be treated by the usual approach to hard exclusive processes in the large-recoil expansion. The scale separations can be systematically performed using recently-developed effective field theory techniques, and for the simplest case of heavy-to-light form factors, relations (19) and (21) give the resulting modifications to heavy-quark symmetry relations appearing at large recoil. The heavy-quark and large-energy scaling laws can be used to inform extrapolations and parameterizations of the form factors, e.g. (33). Knowledge of the form factors can in turn be used to disentangle different contributions to more complicated processes such as $B \rightarrow \pi\pi$.

Acknowledgments

Thanks are due to T. Becher, S. Lee and M. Neubert for collaboration on projects underlying the topics discussed here, and to T. Becher, A. Kronfeld and M. Neubert for useful comments on the manuscript. The author acknowledges interesting conversations with M. Peskin, discussions with J. Dingfelder and L. Hsu on the experimental analysis, and insights from M. Okamoto and J. Shigemitsu on the lattice data. The hospitality of the TRIUMF theory group and KITP (Santa Barbara) is gratefully acknowledged, for brief visits where a portion of this work was completed. Thanks also to the organizers of the KITP workshop “Modern Challenges for Lattice Field Theory”, where an early version of this work was reported. Research supported by the Department of Energy under Grant DE-AC02-76SF00515.

References

- [1] For a review see: M. Neubert, Phys. Rept. **245**, 259 (1994) [hep-ph/9306320].
- [2] G. P. Lepage and S. J. Brodsky, Phys. Rev. D **22**, 2157 (1980).
- [3] A. V. Efremov and A. V. Radyushkin, Phys. Lett. B **94**, 245 (1980).
- [4] C. W. Bauer, S. Fleming and M. E. Luke, Phys. Rev. D **63**, 014006 (2001) [hep-ph/0005275].

- [5] C. W. Bauer, S. Fleming, D. Pirjol and I. W. Stewart, Phys. Rev. D **63**, 114020 (2001) [hep-ph/0011336].
- [6] J. Chay and C. Kim, Phys. Rev. D **65**, 114016 (2002) [hep-ph/0201197].
- [7] M. Beneke, A. P. Chapovsky, M. Diehl and T. Feldmann, Nucl. Phys. B **643**, 431 (2002) [hep-ph/0206152].
- [8] R. J. Hill and M. Neubert, Nucl. Phys. B **657**, 229 (2003) [hep-ph/0211018].
- [9] N. Isgur and M. B. Wise, Phys. Rev. D **42**, 2388 (1990).
- [10] N. Isgur, Phys. Rev. D **43**, 810 (1991).
- [11] A. Szczepaniak, E. M. Henley and S. J. Brodsky, Phys. Lett. B **243**, 287 (1990).
- [12] G. Burdman and J. F. Donoghue, Phys. Lett. B **270**, 55 (1991).
- [13] J. Charles, A. Le Yaouanc, L. Oliver, O. Pene and J. C. Raynal, Phys. Rev. D **60**, 014001 (1999) [hep-ph/9812358].
- [14] M. Beneke and T. Feldmann, Nucl. Phys. B **592**, 3 (2001) [hep-ph/0008255].
- [15] C. W. Bauer, D. Pirjol and I. W. Stewart, Phys. Rev. D **67**, 071502 (2003) [hep-ph/0211069].
- [16] M. Beneke and T. Feldmann, Nucl. Phys. B **685**, 249 (2004) [hep-ph/0311335].
- [17] B. O. Lange and M. Neubert, Nucl. Phys. B **690**, 249 (2004) [hep-ph/0311345].
- [18] R. J. Hill, T. Becher, S. J. Lee and M. Neubert, JHEP **0407**, 081 (2004) [hep-ph/0404217].
- [19] T. Becher, R. J. Hill and M. Neubert, Phys. Rev. D **69**, 054017 (2004) [hep-ph/0308122].
- [20] T. Becher, R. J. Hill, B. O. Lange and M. Neubert, Phys. Rev. D **69**, 034013 (2004) [hep-ph/0309227].
- [21] T. Becher, R. J. Hill and M. Neubert, Phys. Rev. D **72**, 094017 (2005) [hep-ph/0503263].
- [22] See, e.g.: V. L. Chernyak and A. R. Zhitnitsky, Phys. Rept. **112**, 173 (1984), Section 9.
- [23] D. Pirjol and I. W. Stewart, Phys. Rev. D **67**, 094005 (2003) [Erratum-ibid. D **69**, 019903 (2004)] [hep-ph/0211251].
- [24] R. J. Hill, hep-ph/0411073.
- [25] D. Becirevic and A. B. Kaidalov, Phys. Lett. B **478**, 417 (2000) [hep-ph/9904490].
- [26] V. L. Chernyak and I. R. Zhitnitsky, Nucl. Phys. B **345**, 137 (1990).
- [27] M. B. Wise, Phys. Rev. D **45**, 2188 (1992).
- [28] T. M. Yan, H. Y. Cheng, C. Y. Cheung, G. L. Lin, Y. C. Lin and H. L. Yu, Phys. Rev. D **46**, 1148 (1992) [Erratum-ibid. D **55**, 5851 (1997)].

- [29] S. B. Athar *et al.* [CLEO Collaboration], Phys. Rev. D **68**, 072003 (2003) [hep-ex/0304019].
- [30] K. Abe *et al.* [BELLE Collaboration], hep-ex/0408145.
- [31] B. Aubert *et al.* [BABAR Collaboration], hep-ex/0507003.
- [32] G. S. Huang *et al.* [CLEO Collaboration], Phys. Rev. Lett. **94**, 011802 (2005) [hep-ex/0407035].
- [33] J. M. Link *et al.* [FOCUS Collaboration], Phys. Lett. B **607**, 233 (2005) [hep-ex/0410037].
- [34] J. Shigemitsu *et al.*, Nucl. Phys. Proc. Suppl. **140**, 464 (2005) [hep-lat/0408019].
- [35] M. Okamoto *et al.*, Nucl. Phys. Proc. Suppl. **140**, 461 (2005) [hep-lat/0409116].
- [36] P. Ball and R. Zwicky, Phys. Rev. D **71**, 014015 (2005) [hep-ph/0406232].
- [37] C. Aubin *et al.* [Fermilab Lattice Collaboration], Phys. Rev. Lett. **94**, 011601 (2005) [hep-ph/0408306].
- [38] K. M. Foley and G. P. Lepage, Nucl. Phys. Proc. Suppl. **119**, 635 (2003) [hep-lat/0209135].
- [39] G. Burdman, Z. Ligeti, M. Neubert and Y. Nir, Phys. Rev. D **49**, 2331 (1994) [hep-ph/9309272].
- [40] M. Beneke, Y. Kiyo and D. s. Yang, Nucl. Phys. B **692**, 232 (2004) [hep-ph/0402241].
- [41] T. Becher and R. J. Hill, JHEP **0410**, 055 (2004) [hep-ph/0408344].
- [42] T. Becher and R. J. Hill, Phys. Lett. B (in press), [hep-ph/0509090].
- [43] G. Burdman and J. Kambor, Phys. Rev. D **55**, 2817 (1997) [hep-ph/9602353].
- [44] M. Beneke, G. Buchalla, M. Neubert and C. T. Sachrajda, Phys. Rev. Lett. **83**, 1914 (1999) [hep-ph/9905312].
- [45] M. Beneke, G. Buchalla, M. Neubert and C. T. Sachrajda, Nucl. Phys. B **591**, 313 (2000) [hep-ph/0006124].
- [46] C. W. Bauer, D. Pirjol, I. Z. Rothstein and I. W. Stewart, Phys. Rev. D **70**, 054015 (2004) [hep-ph/0401188].
- [47] M. Beneke and M. Neubert, Nucl. Phys. B **675**, 333 (2003) [hep-ph/0308039].
- [48] M. Beneke, G. Buchalla, M. Neubert and C. T. Sachrajda, Phys. Rev. D **72**, 098501 (2005) [hep-ph/0411171].
- [49] C. W. Bauer, D. Pirjol, I. Z. Rothstein and I. W. Stewart, Phys. Rev. D **72**, 098502 (2005) [hep-ph/0502094].
- [50] T. Feldmann and T. Hurth, JHEP **0411**, 037 (2004) [hep-ph/0408188].
- [51] E. Bagan, P. Ball and V. M. Braun, Phys. Lett. B **417**, 154 (1998) [hep-ph/9709243].
- [52] P. Ball, JHEP **9809**, 005 (1998) [hep-ph/9802394].
- [53] F. De Fazio, T. Feldmann and T. Hurth, hep-ph/0504088.